Volume 53
Number 17
7 May 2024
Pages 7243-7644

Dalton Transactions

An international journal of inorganic chemistry

rsc.li/dalton

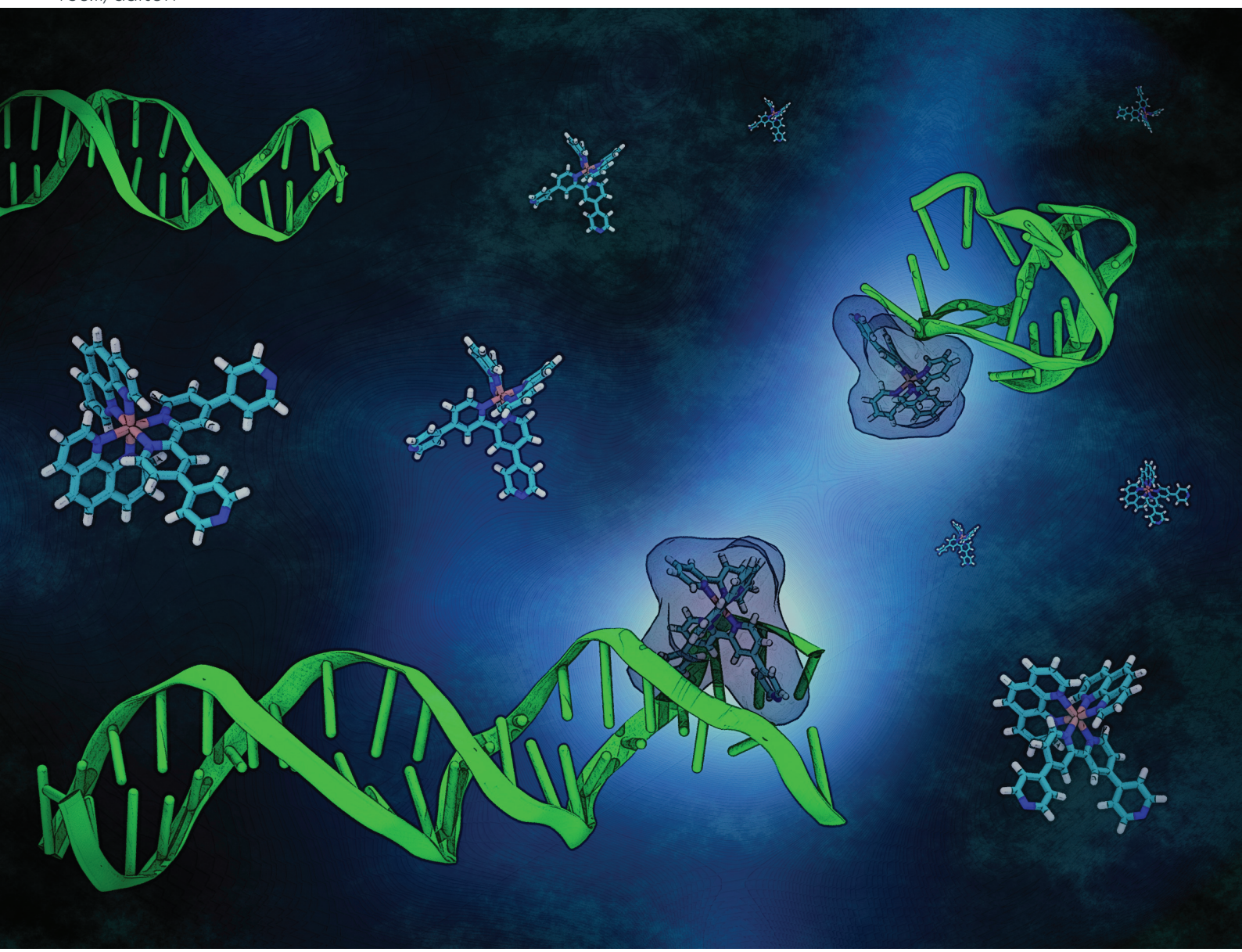

ISSN 1477-9226

ROYAL SOCIETY OF CHEMISTRY

PAPER

Jim A. Thomas *et al.*

Iridium(III)-based minor groove binding complexes as DNA photocleavage agents

Dalton Transactions

ROYAL SOCIETY OF CHEMISTRY

PAPER

View Article Online
View Journal | View Issue

Check for updates

Cite this: *Dalton Trans.*, 2024, **53**, 7282

Iridium(III)-based minor groove binding complexes as DNA photocleavage agents†

Stephen O. Aderinto,[a] Torsten John, ‡[b] Abdulmujeeb Onawole,[c] Raphael Peter Galleh[d] and Jim A. Thomas *[a]

Received 19th January 2024,
Accepted 4th March 2024

DOI: 10.1039/d4dt00171k

rsc.li/dalton

Transition metal complexes containing the qtpy ligand (2′:4,4″:4′,4‴-quaterpyridyl) are known to be DNA intercalators or minor groove binders. In this study, new tricationic iridium(III) complexes of qtpy are reported. Both $[Ir(bpy)_2(qtpy)]^{3+}$ **1** and $[Ir(phen)_2(qtpy)]^{3+}$ **2** display good water solubility as chloride salts. The complexes possess high-energy excited states, which are quenched in the presence of duplex DNA and even by the mononucleotides guanosine monophosphate and adenosine monophosphate. Further studies reveal that although the complexes bind to quadruplex DNA, they display a preference for duplex structures, which are bound with an order of magnitude higher affinities than their isostructural dicationic Ru^{II}-analogues. Detailed molecular dynamics simulations confirm that the complexes are groove binders through the insertion of, predominantly, the qtpy ligand into the minor groove. Photoirradiation of **1** in the presence of plasmid DNA confirms that this class of complexes can function as synthetic photonucleases by cleaving DNA.

Introduction

Following the discovery of the biological activity of cisplatin and its successful development as an anticancer therapy,[1,2] the interaction of transition metal complexes with DNA has been much studied. Initially, Pt^{II} and Pt^{IV} complexes that irreversibly bind DNA formed the basis of research.[3–6] However, with the aim of developing new therapeutic actions, systems capable of reversible intercalation into DNA were soon identified.[7–9]

Over the last few decades, the range of metals used in these studies progressively widened. Fuelled by the discovery of the DNA light-switch complex, $[Ru(LL)_2(dppz)]^{2+}$ (dppz = dipyridylphenazine, LL = 2,2′-bipyridine (bpy) or 1,10-phenanthroline (phen)), a metallo-intercalator that displays an "off-on" metal-to-ligand charge-transfer (MLCT)-based luminescence response to DNA-binding,[10,11] polypyridyl Ru^{II} complexes have attracted a particularly large amount of attention.[12–17] Although research on the light-switch complex and other Ru^{II} analogues first focused on duplex DNA, studies on non-canonical structures such as single-stranded[18] and triplex DNA[19,20] soon emerged. In this context, inspired by the growing interest in quadruplex nucleic acid structures and their myriad putative biological functions, the Thomas group made the first report on a "quadruplex light-switch", identifying a dinuclear complex, $[\{Ru(phen)_2\}_2(tpphz)]^{4+}$ (tpphz = tetrapyrido[3,2-*a*:2′,3′-*c*:3″,2″-*h*:2‴,3‴-*j*]phenazine), that threads into quadruplex loops resulting in a "switched-on" state that is blue-shifted and more intense than the emission induced by its non-intercalative duplex binding;[21] an effect that could also be used to differentiate between duplex and quadruplex structures.[22] Over the following years, a large number of studies on Ru^{II} complexes and their interaction with quadruplexes and other related structures have been reported.[23–27]

More recently, related research into Ir^{III} complexes has developed[28,29] and cyclometalated polypyridyl Ir^{III} metallo-intercalating complexes have proven to be particularly attractive as their photoexcited states are potentially tunable.[30–33] Yet, while such systems have been investigated as therapeutics and cell probes,[34–44] their use is often restricted as – due to their lower cationic charge – they frequently display poor inherent water solubility and lower DNA binding affinities.[45,46] To address this issue, we recently developed routes to dicationic $[Ir(phen)_2(bppz)]^{2+}$ (bppz = benzopyridophenazine) and tricationic $[Ir(bpy)_2(dppz)]^{3+}$, Ir^{III}-based isostructural analogues of the original light-switch complex containing N_5C and N_6 Ir coordination spheres respectively.[47] As might be expected, due to their increased charge, these complexes bind to duplex DNA

[a]*Department of Chemistry, University of Sheffield, Sheffield, S3 7HF, UK. E-mail: james.thomas@sheffield.ac.uk*
[b]*Department of Biological Engineering, Massachusetts Institute of Technology, Cambridge, MA 02139, USA*
[c]*Institute for Molecular Bioscience, The University of Queensland, St. Lucia, QLD 4072, Australia*
[d]*School of Clinical Dentistry, University of Sheffield, Sheffield, S10 2TA, UK*
†Electronic supplementary information (ESI) available. See DOI: https://doi.org/10.1039/d4dt00171k
‡Current address: Max Planck Institute for Polymer Research, Ackermannweg 10, 55128 Mainz, Germany.

with affinities that are two orders of magnitude higher than previously reported monocationic Ir^{III}(dppz)-based systems and are comparable with Ru^{II}(dppz) analogues. Furthermore, the photoexcited states of these two new complexes are very different to their Ru^{II} analogue. In more recent work, $[Ir(phen)_3]^{3+}$ derivatives incorporating extended aromatic moieties were found to possess long-lived intraligand-charge-transfer (ILCT) excited states that offer potential as photosensitisers for photodynamic therapy, PDT.[48]

Although the intercalating/threading ligands employed in all the studies discussed above are planar polyaromatic systems, "non-classical intercalators" consisting of unfused rings are also known.[49,50] Indeed, the Thomas group has identified that Ru^{II} and cyclometallated Ir^{III} complexes incorporating the qtpy ligand (2,2′:4,4″:4′,4‴-quaterpyridyl) can bind to duplex DNA through intercalation *or* groove binding, depending on the metal centre coordinated to the DNA-interacting qtpy ligand.[51] Although these studies initially included cyclometallated Ir^{III} systems, such as $[Ir(phenylpyridine)_2(qtpy)]^+$ and $[Ir(benzo[h]quinoline)_2(qtpy)]^+$, like many other cyclometalated Ir^{III} complexes containing extended aromatic ligands, even their chloride salts displayed very low water solubility so that DNA-binding studies could not be carried out.[51]

Given the increased solubility of N_6Ir^{III} complexes and their potentially novel excited states, we set out to investigate the photophysical and biophysical properties of such metal centres when coordinated to qtpy. Herein, we report new non-cyclometalated, N_6-coordination Ir^{III} complexes and provide an initial investigation into their interaction with a G-quadruplex structure. Our studies reveal that the Ir^{III} complexes presented here are groove binders possessing high-energy excited states capable of photocleaving DNA.

Results and discussion

Synthesis and characterisation

Two new complexes, $[Ir(bpy)_2(qtpy)]^{3+}$ **1** and $[Ir(phen)_2(qtpy)]^{3+}$ **2**, Fig. 1, were synthesised in multistep syntheses starting from $[Ir(bpy)_2Cl_2]PF_6$ and $[Ir(phen)_2Cl_2]PF_6$ *via* $[Ir(bpy)_2(CF_3SO_3)_2]CF_3SO_3$ and $[Ir(bpy)_2(CF_3SO_3)_2]CF_3SO_3$, respectively, through adapted reported methods.[47,52] Specifically, it was found that the final step – the reaction of $[Ir(LL)_2(CF_3SO_3)_2]CF_3SO_3$ (where LL = bpy or phen) with qtpy in EtOH – could only be accomplished through microwave heating over 9–12 hours, reflecting the kinetically inert nature of the Ir^{III} oxidation state – see ESI† for details.

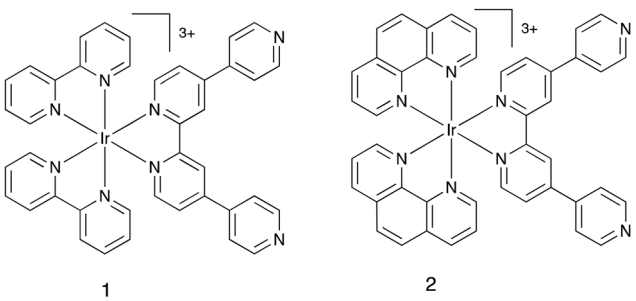

Fig. 1 Newly synthesised complexes **1** and **2**.

To study the DNA binding properties of the complexes, the triflate salts of **1** and **2** were converted to chloride salts and their absorption and emission spectra in aqueous buffer were investigated.

Unlike their cyclometalated, monocationic analogues, $[Ir(ppy)_2(qtpy)]^+$ and $[Ir(bhq)_2(qtpy)]^+$ (ppy = 2-phenylpyridine, bhq = benzo[*h*]quinoline),[51] **1** and **2** display good water solubility. The absorption spectra of the new complexes show characteristic absorption bands[29] in the UV region (200–340 nm) corresponding to ligand-based π–π* transitions and, at lower energies (340–400 nm), MLCT transitions tailing out to 450 nm are observed (see ESI Fig. S1 and S2,† data summarised in Table 1).

In contrast to their isostructural Ru^{II} analogues, the new Ir^{III} complexes displayed vibronically structured emission when photoexcited into their MLCT bands – see ESI Fig. S3 and S4.† These observations are consistent with previous studies indicating that the excited states of such complexes have a large contribution from π–π* states.

The nature of this luminescence is dependent on the ligand attached to the Ir^{III}(qtpy) core. The emission of **1** displays maxima at 458 nm, 489 nm, and 520 nm, and possesses a low energy shoulder that stretches out beyond 600 nm, while the luminescence of **2** shows peaks at 466 nm and 496 nm, with a shoulder at 535 nm that again stretches out to ~610 nm.

DFT calculations

To gain a deeper understanding of the excited state properties of **1** and **2**, they were investigated using quantum chemistry-based methods. The optimised geometries showed that all the complexes form an expected quasi-octahedral coordination geometry with **1** being the most compact – Fig. 2 (see ESI, Table 1†). This is due to the lower steric hindrance of bpy ligands compared to phen.

Generated electrostatic potential maps depicting charge distributions are shown in Fig. 2A These indicate that complex **1** has the most localised positive charge and this is expected as the bpy ligands attached to the Ir^{III} centre have less extended aromatic rings to delocalise over compared to phen.

The calculated frontier orbitals, shown in Fig. 2B, clearly indicate that, although the HOMOs extend over the 5d-orbital

Table 1 Summary of data for the absorption and emission spectra for the chloride salts of complexes **1** and **2** dissolved in water

	λ_{abs} (nm), (ε (M^{-1} cm^{-1}))	λ_{ex} (nm)	λ_{em} (nm)
1	200 (41 710), 250 (35 365), 305 (25 055), 380 (2880)	310	458 (sh), 489, 520 (sh)
2	203 (48 985), 225 (46 595), 273 (46 205), 357 (3805)	315	466, 496, 535 (sh)

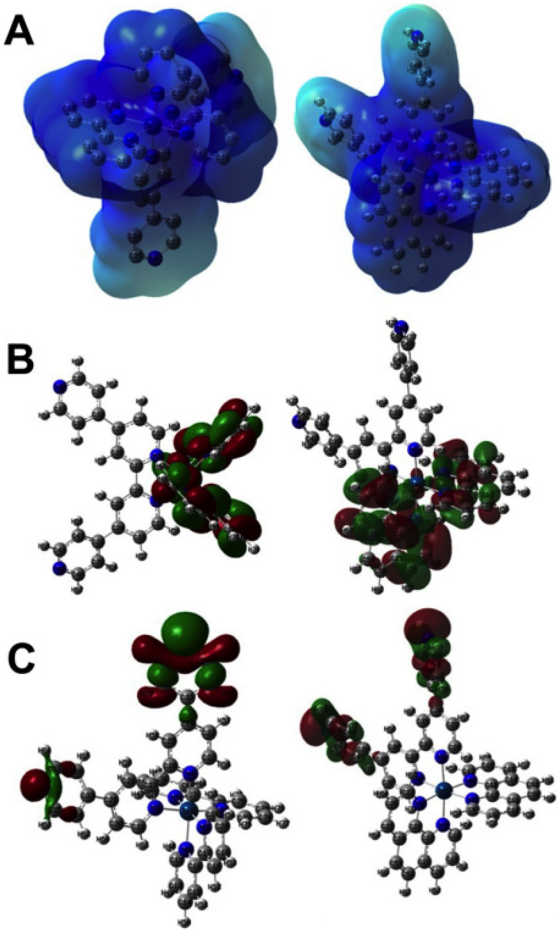

Fig. 2 Results of DFT calculations. (A) Electrostatic potential map of complexes **1** and **2**. (B) Calculated HOMO–1 of each complex. (C) Calculated LUMO–1 of each complex.

on the iridium(III) metal centre, the LUMOs for each complex are exclusively distributed over the qtpy ligands, which is consistent with excited states possessing a contribution from Ir^{III} → qtpy MLCT processes.

Interaction with duplex DNA

To parameterise the binding properties of the two complexes with duplex DNA, luminescent titrations were used. Each complex displayed similar DNA-induced behaviour. Addition of DNA to a solution of the complexes resulted in progressive quenching of luminescence, as illustrated for **2** in Fig. 3 – see ESI† for similar data on **1** (Fig. S5†). These observations are in stark contrast to their isostructural Ru^{II} analogues $[Ru(bpy)_2(qpty)]^{2+}$ and $[Ru(phen)_2(qpty)]^{2+}$ whose emission is unaffected by addition of DNA.[51,53,54]

The changes observed for **1** and **2** were fit to the McGhee-von Hippel model for non-cooperative binding[55] to produce the binding parameters presented in Table 2 (see ESI Fig. S6†). The resulting estimated binding affinities for **1** and **2** with duplex DNA are significantly larger than that obtained for its

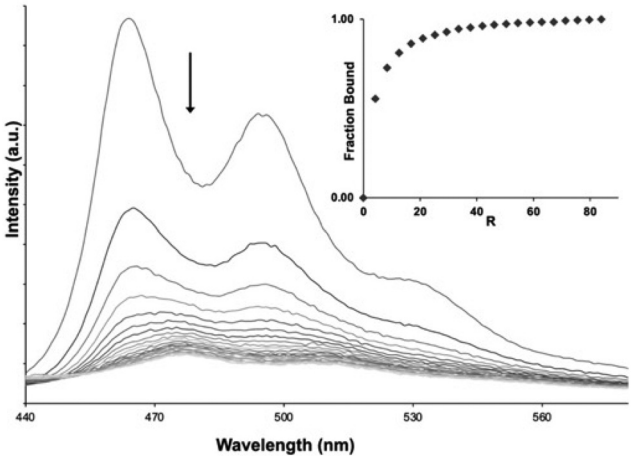

Fig. 3 Example of changes in the luminescence of a buffered aqueous 100 μM solution of **2** on addition of calf thymus-DNA, CT-DNA, up to excess. Inset: binding curve constructed from these data, *R* is the binding ratio.

Table 2 Summary of duplex DNA and quadruplex DNA binding parameters (K_b) for new complexes estimated from fits to the McGhee–von Hippel model for non-cooperative binding and a one-set-of-sites binding model respectively. HTS = human telomere sequence

Complex	K_b (M^{-1}) for duplex (site size)	K_b (M^{-1}) for HTS
1	3.7×10^6 (8 bp)	1.68×10^5
2	1.5×10^6 (8 bp)	4.5×10^5

isostructural Ru^{II}-dications, with K_b for **1** being more than an order of magnitude higher[53] than that for $[Ru(bpy)_2(qtpy)]^{2+}$ – indicating that the increased charge of the Ir^{III} complexes makes an appreciable contribution to this interaction. Interestingly, fits to the McGhee-von Hippel model for both complexes reveal a larger site size of 8 bp than that observed for most metallo-intercalators, which typically display site sizes of ~3 bp, suggesting that they display some sequence selectivity.

The decreasing emission of **1** and **2** on addition of DNA is consistent with the kind of photo-induced redox processes frequently observed with metal complexes possessing photo-oxidising excited states.[56–58] Indeed, we have previously reported on a dinuclear Ru^{II}-complex containing electron deficient tetraazaphenanthrene ligands[59,60] as well as organic cationic intercalators[61–63] that exhibit similar behaviour. In such systems, quenching occurs on binding to DNA as their high energy excited states oxidise specific base sites within the duplex. Usually this process involves guanine sites, as they have the most accessible one-electron oxidation (1.29 V *vs.* NHE), but if excited states are sufficiently energetic photo-oxidation of adenine (2.03 V *vs.* NHE) can also occur.[61,64,65] To investigate this question, the effect of increasing concentrations of nucleotide monophosphates on the emission spectrum of **1** and **2** was explored.

Emission quenching by nucleotide phosphates

The addition of either guanosine monophosphate (GMP) or adenosine monophosphate (AMP) led to emission quenching of solutions of **1** and **2**, as the examples in Fig. 4 and Fig. S7 (see ESI†) demonstrate. This confirms that the excited-states of these complexes can photo-oxidise both AMP and GMP. Classical linear Stern–Volmer plots are observed for the quenching of **1** by GMP and AMP and **2** with GMP (see Fig. 4B); however, the plots associated with the addition of AMP to **2** display distinctive positive curvatures (Fig. 4D).

This phenomenon is indicative of static quenching, likely due to a ground state interaction between the complex and AMP. Certainly, previous studies have shown that complexes containing extended aromatic ligands, including qtpy, can interact with nucleotides through π–π stacking interactions.[59,66–69] In this case, it seems the extended aromatic surfaces of the phen ligand are required for this interaction.

Taken together, these experiments and the data from the DNA binding studies indicate that the complexes interact with duplex DNA and can photo-oxidise both A and G sites within a duplex. These studies were then extended to investigate a representative G-quadruplex DNA sequence.

Binding to quadruplex DNA

In recent decades there has been an explosion of interest in the structure and function of G-rich sequences capable of forming quadruplexes.[70–73] These studies have revealed putative roles for quadruplex DNA in a wide range of cellular processes including fundamental genetics, genetic disease, and ageing.[74–82] A much-studied example is provided by telomeric DNA.

Although telomere sequences found at the end of chromosomes[83] are single-stranded, they are known to fold into quadruplex structures.[84–88] Significantly, telomeres have a role in defining the Hayflick limits for cell division, as each cell division results in shortening of the telomere sequence, until a critical length is reached, and senescence is triggered.[82,89–92] It is also established that telomere length maintenance is a key marker of cell immortalisation in carcinogenesis.[93–95] For these reasons, methods to selectively bind to telomeric quadruplexes[96–99] and/or shorten telomere length in cancer cells have been investigated.[27,59,100–103] Given that such studies have included transition metal complexes as binding substrates,[25,104] and previous work within the Thomas group has identified Ru^{II} complexes that bind to quadruplex-folded human telomere sequence (HTS) with high affinities,[21,22,105,106] analogous experiments were carried out with **1** and **2**. These were of particular interest as a very recent report from the Keyes group[107] has shown that a Ru^{II}-complex containing a ligand derived from phen-DC3[108] – a high-affinity quadruplex-binding substrate[109] that has some structural similarities to qtpy – actually disrupts quadruplex structures. The addition of HTS to solutions of **1** and **2** also resulted in quenching, Fig. 5 and ESI Fig. S8A,† with progressive addition of quadruplex.

Again, the changes in emission were used to estimate the binding affinities of the complexes to HTS. In this case, the data was best fitted to a one-set-of-sites binding model – Fig. 5B, ESI Fig. S8B† and Table 2. In both cases, the estimated K_b values for binding to quadruplex were lower than those for duplex DNA, however this difference was much larger for **1** – where K_b for duplex is over $\times 20 K_b$ of that of the quadruplex – than for **2**, where the difference is only three-fold.

The effect of the complexes on the stability of the folded quadruplex was explored with circular dichroism, CD. Although the racemic mixtures of each complex are not active themselves, the folded quadruplex is chiral and has a characteristic CD signature, with a negative peak at 260 nm and positive peak maximum at 290 nm.[110] As illustrated in Fig. 6 and ESI Fig. S9,† it was found that even after addition of excess complex, neither **1** nor **2** produced any real change in the CD of the folded oligonucleotide, indicating that unlike the structures reported by the Keyes group, complexes **1** and **2** do not

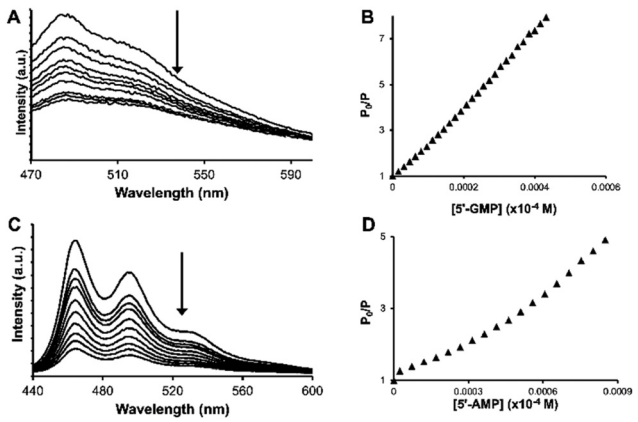

Fig. 4 Examples of the aqueous solution quenching of luminescence of complexes by nucleotides. (A) Change in emission from an aqueous solution of **1** upon successive addition of 5′-GMP. (B) Stern–Volmer plot derived from data shown in A. (C) Change in emission from an aqueous solution of **2** upon successive addition of 5′-AMP (D) Nonlinear Stern–Volmer plot derived from data shown in C.

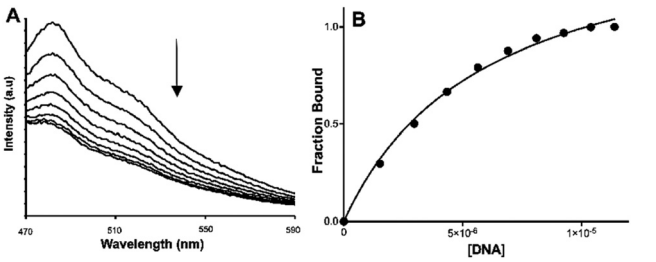

Fig. 5 (A) Details of the luminescence response induced through progressive addition of 0.85 μM of quadruplex folded HTS to complex **1**. (B) Binding curve for **1** with HTS constructed using emission data – continuous line shows fitting to binding to one-set-of-sites.

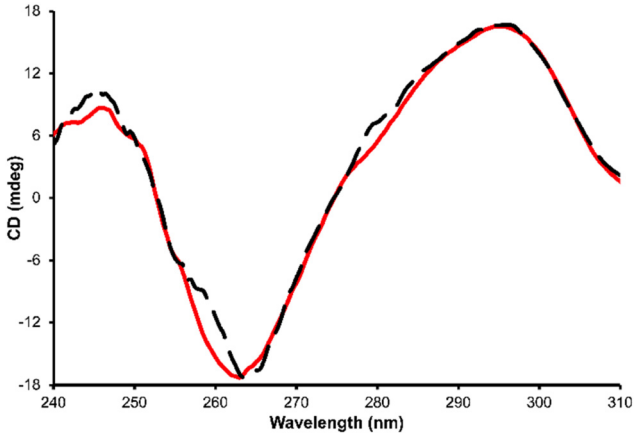

Fig. 6 CD spectrum of 5.65 μM HTS (black broken line) and in the presence of 37.36 μM of **2** (red line) in PBS buffer, pH 7.41 at 25 °C.

disrupt the folded structure on interacting with the quadruplex.

Molecular dynamics studies

Although we have previously used molecular dynamics (MD) simulations to provide insights into the quadruplex DNA binding properties of dinuclear Ru^{II} complexes,[106] simulations on the interaction of metal complexes with DNA – particularly noncanonical structures – are still very rare. While our previous studies had shown that qtpy complexes can interact with duplex DNA through intercalation or groove binding, further insights into the interactions of **1** and **2** with the two different DNA structures were sought through detailed MD simulations.

Geometry optimised structures of **1** and **2** were first parameterised and then simulated in Amber and Ambertools22[111] (see ESI† for details); likewise, the CT-DNA used in experiments was modelled by a DNA duplex (B-form, sequence: AATTGGCCAATTGGCCAATT), and for the G-quadruplex, the unimolecular 22-nt human telomeric DNA, d[AGGG-$(TTAGGG)_3$] structure[112] from the Protein Data Bank (PDB entry: 143D) was used (see ESI† for full details). The MD simulations were analysed to identify dominant binding motifs of the complexes to the DNA structures. Clustering of the simulation trajectories was performed over all replicates for each system. In the simulations with the duplex, two types of interaction common to both complexes were observed. The first was an end-stacking interaction onto the blunt ends of the duplex (see ESI, Fig. S10 and S11†). Such interactions have been observed in X-ray structures of polypyridyl Ru^{II} systems before. The second common binding motif is more likely to be representative of what occurs experimentally on interaction with CT-DNA as these are much longer and statistically less ends prominent. In this arrangement, illustrated by the interaction of **1** with duplex DNA depicted in Fig. 7A, the qtpy ligand is inserted parallel to the minor groove, with its ring

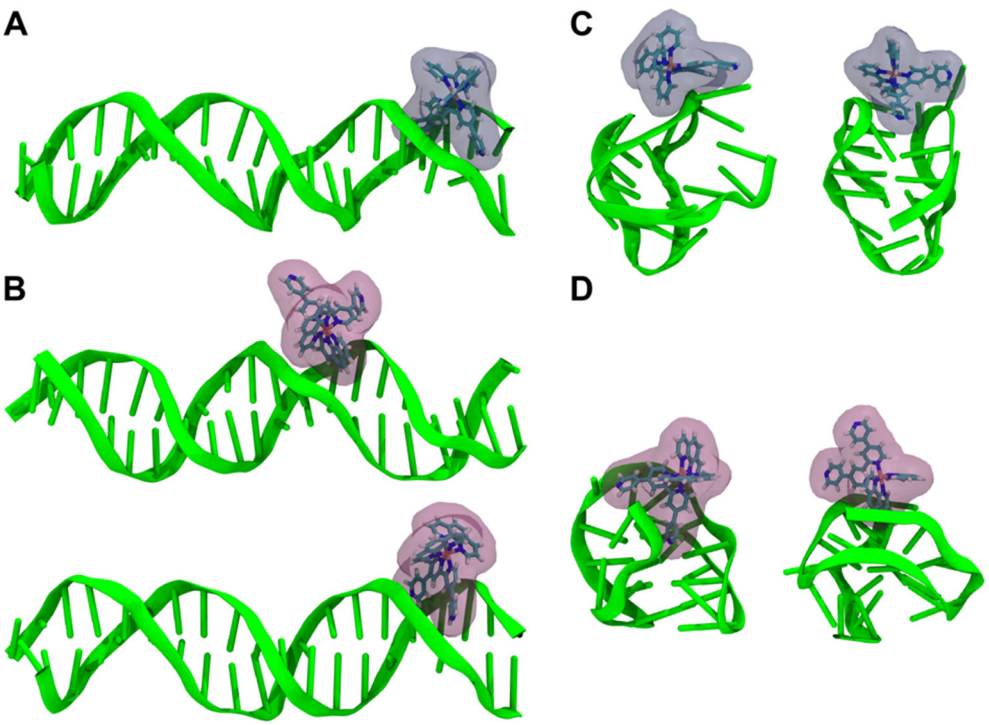

Fig. 7 MD simulations for the interaction of complexes **1** and **2** with duplex and quadruplex DNA. (A) Minor groove binding motif of complex **1** to duplex DNA. (B) Dominant binding modes of complex **2** to duplex DNA, showing "minor facial" binding of phen ligands (top) and minor groove binding with qtpy inserted into groove (bottom). (C) Dominant end-pasting motifs for the interaction of **1** with quadruplex-folded HTS. (D) Dominant end-pasting motifs for the interaction of **2** with quadruplex-folded HTS.

system tracking the curvature of the double helix. Complex **2** is seen to bind into the duplex in a similar manner to that observed for **1** (Fig. 7B) with the qtpy ligand inserted parallel to the groove. Thus, our simulations indicate that both **1** and **2** are minor groove binders. Complex **2** also displayed a second dominant binding geometry within the minor groove in which a phen ligand inserts into the groove (Fig. 7B). This "semi-intercalation" motif has been observed in several crystal structures of $[Ru(LL)_2(dppz)]^{2+}$ (where LL = phenanthroline or 1,4,5,8-tetraazaphenanthrene)[113–115] bound to duplexes. Related studies involving HTS resulted in a more flexible and a more diverse set of structures.

For both **1** and **2**, the simulations resulted in several binding poses with folded HTS that are represented in Fig. 7C and D. For **1**, the metal complex either sits externally to the groove of the quadruplex or in a more intimate interaction with the lateral loop end of the folded structure. In the latter structure, the qpty ligand is orientated with the cleft defined by the two loops and uncoordinated pyridyl rings are parallel with A residues in each of the lateral loop. Binding motifs involving complex **2** also involved external groove binding as well as a contrasting close interaction involving qtpy. In this case, the complex was found at the opposite, diagonal loop end of the folded quadruplex binding into its wide groove in a manner that is much closer to the duplex groove binding motif. Next, to gain quantitative insights into the relative binding strengths with the two different DNA structures, analysis was extended to investigate the solvent accessibility of interacting surfaces and the comparative flexibility of the binding motifs. The solvent accessible surface area (SASA) of the Ir(III)-complexes, obtained using the LCPO algorithm,[116] was calculated for the initial 10 ns simulation time and the last 100 ns simulation time and averaged for the respective simulations of complex-duplex and complex-G-quadruplex and changes in SASA were used to qualitatively compare the binding affinity of the different complexes to the DNA structures (Fig. 8A).

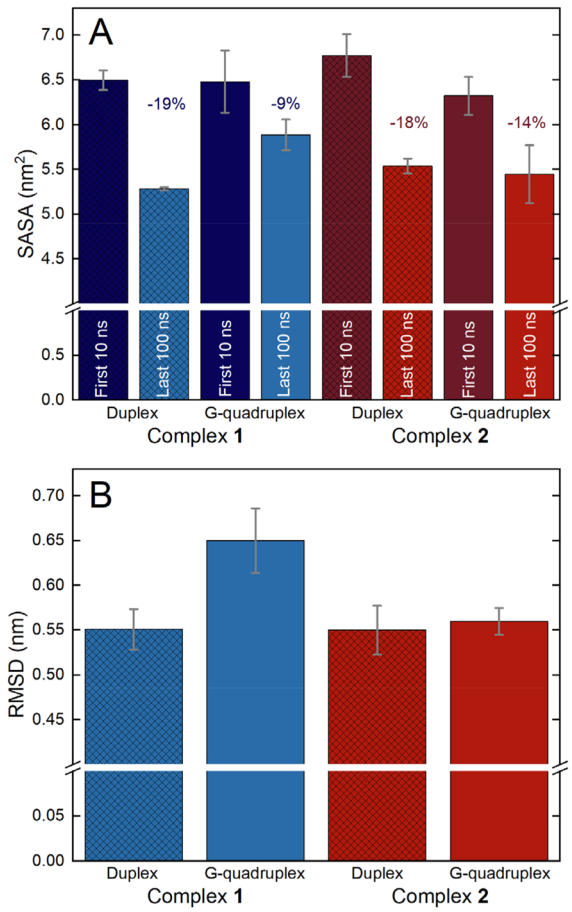

Fig. 8 (A) The SASA of the Ir(III)-complexes was calculated using the LCPO algorithm. Error bars indicate standard errors of the mean. SASAs were determined for the first 10 ns simulation time to reflect the initial SASA of the complex in solvent, and for the last 100 ns simulation time to reflect the DNA-bound states. Reported values are averages over all repetitions. The decrease in SASA upon DNA binding is shown. (B) The RMSD of the Ir(III)-complexes was calculated for the last 100 ns simulation time to reflect the DNA-bound states. Error bars indicate standard errors of the mean. Reported values are averages over all replicates.

These figures showed larger changes in SASA for the interactions with duplex over G-quadruplex for both complexes, but this was particularly apparent for complex **1**.

To further probe the interaction of the complexes with the two DNA structures, their root mean square displacements (RMSD) were calculated for the last 100 ns simulation time and averaged for the respective simulations of complex-duplex and complex-G-quadruplex binding to quantify the flexibility of the different complexes to the DNA structures (Fig. 8B). These calculations reveal that while complex **2** showed similar flexibility when bound to duplex and G-quadruplex, complex **1** was appreciably more rigidly bound to the duplex than the G-quadruplex structure.

Taken together, the SASA and RMSD calculations indicate that complex **1** displays more pronounced binding selectivity than complex **2**, as it appears to bind more tightly to duplex than quadruplex; a conclusion that agrees with the experimental observations.

DNA photocleavage

Given that the excited states of **1** and **2** are quenched on binding to DNA, it seemed likely they were capable of photodamaging nucleotides. Therefore, photocleavage experiments with plasmid DNA were carried out using complex **1** as the representative example.

The photonuclease activity of **1** was assessed using the supercoiled pBR322 plasmid under both unilluminated and illuminated conditions. In the dark, no cleavage was observed. However, as illustrated by Fig. 9, subsequent photoirradiation of the supercoiled form leads to the generation of relaxed singly nicked plasmid in a concentration-dependent manner. At higher complex loading, or extended illumination periods further degradation of the DNA through double nicking is evident, confirming that this class of complexes offer promise as photocleavage agents.

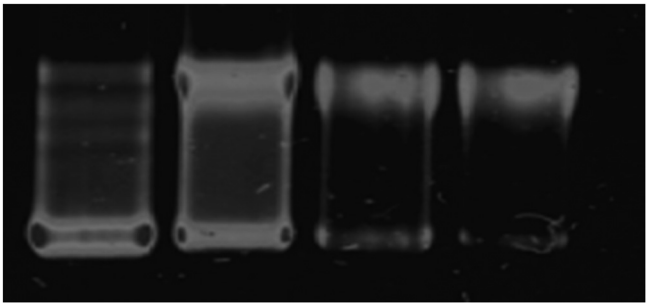

Fig. 9 Photocleavage of supercoiled pBR322 DNA by **1** in 5 mM Tris, 25 mM NaCl buffer. (Right to left) lane 1: DNA control; lane 2: DNA + 10 μM complex **1**; lane 3: DNA + 20 μM complex **1**; lane 4: DNA + 30 μM complex **1**. Illumination conditions: λ_{ex} = 365 nm, 125 mV, 10 minutes.

Conclusions

Although there is a huge amount of work on polypyridyl Ru^{II} complexes as metallointercalators, very few studies have investigated the potential of such systems as groove binders, even though minor groove binders often possess higher affinities and selectivity. Furthermore, there has been no work on tricationic N_6Ir^{III} complexes in this context. Herein, we demonstrate that these relatively easily accessed class of compounds offer an opportunity to develop systems that can bind to DNA structures with affinities that are considerably higher than their Ru^{II} analogues. The photophysical properties of this class of compounds are very different to equivalent Ru^{II} and conventional cyclometallated Ir^{III} complexes, as they can display distinctive photonuclease activity as they are photoredox quenched by both G and A-steps.

In future reports we will explore the interaction of this class of complexes with other biomolecules. Although these compounds possess higher charge than their Ru^{II} analogues, which can often decrease cell-membrane permeance, this is not always the case;[105,117,118] therefore, their cell uptake and potential as novel phototherapeutics will also be investigated and assessed.

Author contributions

The study was designed and conceptualised by S. O. A. and J. A. T. Synthesis and experimental characterisation were performed by S. O. A. Biophysical studies were carried out by S. O. A. and R. P. G. Geometry optimisation and DFT to study excited states were performed and analysed by A. O. Force field parameterisation, including DFT, and MD simulations were performed and analysed by T. J. The results were discussed and interpreted by S. O. A., T. J., A. O. and J. A. T. The research was supervised by J. A. T. The first draft of the manuscript was written by J. A. T. and revised by S. O. A. and T. J.

Conflicts of interest

There are no conflicts to declare.

Acknowledgements

S. A. O. is grateful for the award of a University of Sheffield Research Scholarship. T. J. thanks Prof. Dr. Mark Bathe (MIT, Cambridge, MA, USA) for his mentorship and project funding. T. J. was supported by the National Science Foundation (NSF, CCF-1956054) and the Office of Naval Research (ONR, N00014-21-1-4013), and acknowledges financial support from the Alexander von Humboldt Foundation through a Feodor-Lynen Research Fellowship. The authors acknowledge the MIT SuperCloud and Lincoln Laboratory Supercomputing Center as well as the MIT Engaging Cluster for providing HPC resources that have contributed to the research results reported within this work.

References

1 B. Rosenberg, L. Van Camp, J. E. Trosko and V. H. Mansour, *Nature*, 1969, **222**, 385–386.
2 S. Ghosh, *Bioorg. Chem.*, 2019, **88**, 102925.
3 D. Wang, *Nat. Rev. Drug Discovery*, 2005, **4**, 307–320.
4 S. Dilruba and G. V. Kalayda, *Cancer Chemother. Pharmacol.*, 2016, **77**, 1103–1124.
5 K. M. Deo, D. L. Ang, B. McGhie, A. Rajamanickam, A. Dhiman, A. Khoury, J. Holland, A. Bjelosevic, B. Pages, C. Gordon and J. R. Aldrich-Wright, *Coord. Chem. Rev.*, 2018, **375**, 148–163.
6 T. C. Johnstone, K. Suntharalingam and S. J. Lippard, *Chem. Rev.*, 2016, **116**, 3436–3486.
7 K. W. Jennette, S. J. Lippard, G. A. Vassiliades and W. R. Bauer, *Proc. Natl. Acad. Sci. U. S. A.*, 1974, **71**, 3839–3843.
8 R. W.-Y. Sun, A. L.-F. Chow, X.-H. Li, J. J. Yan, S. S.-Y. Chui and C.-M. Che, *Chem. Sci.*, 2011, **2**, 728–736.
9 B. J. Pages, F. Li, P. Wormell, D. L. Ang, J. K. Clegg, C. J. Kepert, L. K. Spare, S. Danchaiwijit and J. R. Aldrich-Wright, *Dalton Trans.*, 2014, **43**, 15566–15575.
10 A. E. Friedman, J. K. Barton, J. C. Chambron, J. P. Sauvage, N. J. Turro and J. K. Barton, *J. Am. Chem. Soc.*, 1990, **112**, 4960–4962.
11 C. Hiort, P. Lincoln and B. Nordén, *J. Am. Chem. Soc.*, 1993, **115**, 3448–3454.
12 B. M. Zeglis, V. C. Pierre and J. K. Barton, *Chem. Commun.*, 2007, **7345**, 4565–4579.
13 M. R. Gill and J. A. Thomas, *Chem. Soc. Rev.*, 2012, **41**, 3179–3192.
14 A. W. McKinley, P. Lincoln and E. M. Tuite, *Coord. Chem. Rev.*, 2011, **255**, 2676–2692.
15 F. E. Poynton, S. A. Bright, S. Blasco, D. C. Williams, J. M. Kelly and T. Gunnlaugsson, *Chem. Soc. Rev.*, 2017, **46**, 7706–7756.
16 F. Heinemann, J. Karges and G. Gasser, *Acc. Chem. Res.*, 2017, **50**, 2727–2736.
17 M. Lin, S. Zou, X. Liao, Y. Chen, D. Luo, L. Ji and H. Chao, *Chem. Commun.*, 2021, **57**, 4408–4411.

18 C. G. Coates, J. J. McGarvey, P. L. Callaghan, M. Coletti and J. G. Hamilton, *J. Phys. Chem. B*, 2001, **105**, 730–735.
19 S. D. Choi, M. S. Kim, S. K. Kim, P. Lincoln, E. Tuite and B. Nordén, *Biochemistry*, 1997, **36**, 214–223.
20 M. N. Peng, Z. Y. Zhu and L. F. Tan, *Inorg. Chem.*, 2017, **56**, 7312–7315.
21 C. Rajput, R. Rutkaite, L. Swanson, I. Haq and J. A. Thomas, *Chem. – Eur. J.*, 2006, **12**, 4611–4619.
22 T. Wilson, M. P. Williamson and J. A. Thomas, *Org. Biomol. Chem.*, 2010, **8**, 2617–2621.
23 K. McQuaid, J. P. Hall, L. Baumgaertner, D. J. Cardin and C. J. Cardin, *Chem. Commun.*, 2019, **55**, 9116–9119.
24 K. T. McQuaid, S. Takahashi, L. Baumgaertner, D. J. Cardin, N. G. Paterson, J. P. Hall, N. Sugimoto and C. J. Cardin, *J. Am. Chem. Soc.*, 2022, **144**, 5956–5964.
25 E. Palma, J. Carvalho, C. Cruz and A. Paulo, *Pharmaceuticals*, 2021, **14**, 605.
26 J. Jiang, T. Teunens, J. Tisaun, L. Denuit and C. Moucheron, *Molecules*, 2022, **27**, 1541.
27 M. Gillard, G. Piraux, M. Daenen, M. Abraham, L. Troian-Gautier, L. Bar, H. Bonnet, F. Loiseau, H. Jamet, J. Dejeu, E. Defrancq and B. Elias, *Chem. – Eur. J.*, 2022, **28**, e20220225.
28 I. M. Dixon, J.-P. Collin, J.-P. Sauvage, L. Flamigni, S. Encinas and F. Barigelletti, *Chem. Soc. Rev.*, 2000, **29**, 385–391.
29 L. Flamigni, A. Barbieri, C. Sabatini, B. Ventura and F. Barigelletti, *Top. Curr. Chem.*, 2007, **281**, 143–203.
30 S. Lamansky, P. Djurovich, D. Murphy, F. Abdel-Razzaq, H. E. Lee, C. Adachi, P. E. Burrows, S. R. Forrest and M. E. Thompson, *J. Am. Chem. Soc.*, 2001, **123**, 4304–4312.
31 T. Sajoto, P. I. Djurovich, A. Tamayo, M. Yousufuddin, R. Bau, M. E. Thompson, R. J. Holmes and S. R. Forrest, *Inorg. Chem.*, 2005, **44**, 7992–8003.
32 S. Ladouceur and E. Zysman-Colman, *Eur. J. Inorg. Chem.*, 2013, **2013**, 2985–3007.
33 Ł. Skórka, M. Filapek, L. Zur, J. G. Małecki, W. Pisarski, M. Olejnik, W. Danikiewicz and S. Krompiec, *J. Phys. Chem. C*, 2016, **120**, 7284–7294.
34 L. Lu, L. J. Liu, W. C. Chao, H. J. Zhong, M. Wang, X. P. Chen, J. J. Lu, R. N. Li, D. L. Ma and C. H. Leung, *Sci. Rep.*, 2015, **5**, 14544–14549.
35 J. J. Cao, C. P. Tan, M. H. Chen, N. Wu, D. Y. Yao, X. G. Liu, L. N. Ji and Z. W. Mao, *Chem. Sci.*, 2016, **8**, 631–640.
36 J. Kasparkova, A. Hernández-García, H. Kostrhunova, M. Goicuría, V. Novohradsky, D. Bautista, L. Markova, M. D. Santana, V. Brabec and J. Ruiz, *J. Med. Chem.*, 2024, **67**, 691–708.
37 K. K. W. Lo, *Acc. Chem. Res.*, 2015, **48**, 2985–2995.
38 Q. Zhao, C. Huang and F. Li, *Chem. Soc. Rev.*, 2011, **40**, 2508–2524.
39 X. Tian, C. De Pace, L. Ruiz-Perez, B. Chen, R. Su, M. Zhang, R. Zhang, Q. Zhang, Q. Wang, H. Zhou, J. Wu, Z. Zhang, Y. Tian and G. Battaglia, *Adv. Mater.*, 2020, **32**, e2003901.
40 C. Caporale, C. A. Bader, A. Sorvina, K. D. M. MaGee, B. W. Skelton, T. A. Gillam, P. J. Wright, P. Raiteri, S. Stagni, J. L. Morrison, S. E. Plush, D. A. Brooks and M. Massi, *Chem. – Eur. J.*, 2017, **23**, 15666–15679.
41 A. H. Day, M. H. Übler, H. L. Best, E. Lloyd-Evans, R. J. Mart, I. A. Fallis, R. K. Allemann, E. A. H. H. Al-Wattar, N. I. Keymer, N. J. Buurma and S. J. A. A. Pope, *Chem. Sci.*, 2020, **115**, 195–198.
42 P. Y. Ho, C. L. Ho and W. Y. Wong, *Coord. Chem. Rev.*, 2020, **413**, 213267.
43 H. Yuan, Z. Han, Y. Chen, F. Qi, H. Fang, Z. Guo, S. Zhang and W. He, *Angew. Chem., Int. Ed.*, 2021, **60**, 8174–8181.
44 B. Das, S. Gupta, A. Mondal, K. J. Kalita, A. I. Mallick and P. Gupta, *J. Med. Chem.*, 2023, **66**, 15550–15563.
45 K. K. W. Lo, C. K. Chung and N. Zhu, *Chem. – Eur. J.*, 2006, **12**, 1500–1512.
46 F. Shao, B. Elias, W. Lu and J. K. Barton, *Inorg. Chem.*, 2007, **46**, 10187–10199.
47 S. Stimpson, D. R. Jenkinson, A. Sadler, M. Latham, A. Wragg, A. J. H. M. Meijer and J. A. Thomas, *Angew. Chem., Int. Ed.*, 2015, **54**, 3000–3003.
48 L. Wang, S. Monro, P. Cui, H. Yin, B. Liu, C. G. Cameron, W. Xu, M. Hetu, A. Fuller, S. Kilina, S. A. McFarland and W. Sun, *ACS Appl. Mater. Interfaces*, 2019, **11**, 3629–3644.
49 L. Strekowski and B. Wilson, *Mutat. Res., Fundam. Mol. Mech. Mutagen.*, 2007, **623**, 3–13.
50 R. D. Snyder, D. E. Ewing and L. B. Hendry, *Environ. Mol. Mutagen.*, 2004, **44**, 163–173.
51 H. Ahmad, A. Wragg, W. Cullen, C. Wombwell, A. J. H. M. Meijer and J. A. Thomas, *Chem. – Eur. J.*, 2014, **20**, 3089–3096.
52 M. Pandrala, F. Li, L. Wallace, P. J. Steel, B. Moore II, J. Autschbach, J. G. Collins and F. R. Keene, *Aust. J. Chem.*, 2013, **66**, 1065–1073.
53 R. J. Morgan, S. Chatterjee, A. D. Baker and T. C. Strekas, *Inorg. Chem.*, 1991, **30**, 2687–2692.
54 H. Ahmad, D. Ghosh and J. A. Thomas, *Chem. Commun.*, 2014, **50**, 3859–3861.
55 J. D. McGhee and P. H. von Hippel, *J. Mol. Biol.*, 1974, **86**, 469–489.
56 B. Elias and A. Kirsch-De Mesmaeker, *Coord. Chem. Rev.*, 2006, **250**, 1627–1641.
57 L. Herman, S. Ghosh, E. Defrancq and A. Kirsch-De Mesmaeker, *J. Phys. Org. Chem.*, 2008, **21**, 670–681.
58 J. Ghesquiere, S. Le Gac, L. Marcelis, C. Moucheron and A. Kirsch-De Mesmaeker, *Curr. Top. Med. Chem.*, 2012, **12**, 185–196.
59 S. A. Archer, A. Raza, F. Dröge, C. Robertson, A. J. Auty, D. Chekulaev, J. A. Weinstein, T. Keane, A. J. H. M. Meijer, J. W. Haycock, S. Macneil and J. A. Thomas, *Chem. Sci.*, 2019, **10**, 3502–3513.
60 A. Raza, S. A. Archer, S. D. Fairbanks, K. L. Smitten, S. W. Botchway, J. A. Thomas, S. MacNeil and J. W. Haycock, *J. Am. Chem. Soc.*, 2020, **142**, 4639–4647.

61 T. Phillips, I. Haq, A. J. H. M. Meijer, H. Adams, I. Soutar, L. Swanson, M. J. Sykes and J. A. Thomas, *Biochemistry*, 2004, **43**, 13657–13665.
62 T. Phillips, C. Rajput, L. Twyman, I. Haq and J. A. Thomas, *Chem. Commun.*, 2005, **44**, 4327–4329.
63 T. Phillips, I. Haq and J. A. Thomas, *Org. Biomol. Chem.*, 2011, **9**, 3462–3470.
64 C. A. M. Seidel, A. Schulz and M. H. M. Sauer, *J. Phys. Chem.*, 1996, **100**, 5541–5553.
65 F. A. Baptista, D. Krizsan, M. Stitch, I. V. Sazanovich, I. P. Clark, M. Towrie, C. Long, L. Martinez-Fernandez, R. Improta, N. A. P. Kane-Maguire, J. M. Kelly and S. J. Quinn, *J. Am. Chem. Soc.*, 2021, **143**, 14766–14779.
66 H. Ahmad, B. W. Hazel, A. J. H. M. Meijer, J. A. Thomas and K. A. Wilkinson, *Chem. – Eur. J.*, 2013, **19**, 5081–5087.
67 A. M. Agafontsev, A. Ravi, T. A. Shumilova, A. S. Oshchepkov and E. A. Kataev, *Chem. – Eur. J.*, 2019, **25**, 2684–2694.
68 A. M. Agafontsev, T. A. Shumilova, A. S. Oshchepkov, F. Hampel and E. A. Kataev, *Chem. – Eur. J.*, 2020, **26**, 9991–9997.
69 L. Catti, R. Sumida and M. Yoshizawa, *Coord. Chem. Rev.*, 2022, **460**, 214460.
70 P. Baumann, *Nat. Struct. Mol. Biol.*, 2005, **12**, 832–833.
71 G. N. Parkinson, in *Quadruplex Nucleic Acids*, ed. S. Neidle and S. Balasubramanian, 2007, pp. 1–30.
72 J. L. Huppert, *Chem. Soc. Rev.*, 2008, **37**, 1375–1384.
73 E. Y. N. Lam, D. Beraldi, D. Tannahill and S. Balasubramanian, *Nat. Commun.*, 2013, **4**, 1796.
74 D. Rhodes and H. J. Lipps, *Nucleic Acids Res.*, 2015, **43**, 8627–8637.
75 D. Varshney, J. Spiegel, K. Zyner, D. Tannahill and S. Balasubramanian, *Nat. Rev. Mol. Cell Biol.*, 2020, **21**, 459–474.
76 T. Tian, Y. Q. Chen, S. R. Wang and X. Zhou, *Chem*, 2018, **4**, 1314–1344.
77 R. Hänsel-Hertsch, D. Beraldi, S. V. Lensing, G. Marsico, K. Zyner, A. Parry, M. Di Antonio, J. Pike, H. Kimura, M. Narita, D. Tannahill and S. Balasubramanian, *Nat. Genet.*, 2016, **48**, 1267–1272.
78 Y. Wang, J. Yang, A. T. Wild, W. H. Wu, R. Shah, C. Danussi, G. J. Riggins, K. Kannan, E. P. Sulman, T. A. Chan and J. T. Huse, *Nat. Commun.*, 2019, **10**, 1–14.
79 R. Simone, P. Fratta, S. Neidle, G. N. Parkinson and A. M. Isaacs, *FEBS Lett.*, 2015, **589**, 1653–1668.
80 A. Malousi, A. Z. Andreou, E. Georgiou, G. Tzimagiorgis, L. Kovatsi and S. Kouidou, *Epigenetics*, 2018, **13**, 808–821.
81 D. Liano, S. Chowdhury and M. Di Antonio, *J. Am. Chem. Soc.*, 2021, **143**, 20988–21002.
82 M. A. Blasco, *Nat. Chem. Biol.*, 2007, **3**, 640–649.
83 E. H. Blackburn, *Nature*, 2000, **408**, 53–56.
84 K. Paeschke, T. Simonsson, J. Postberg, D. Rhodes and H. J. Lipps, *Nat. Struct. Mol. Biol.*, 2005, **12**, 847–854.
85 K. Paeschke, S. Juranek, T. Simonsson, A. Hempel, D. Rhodes and H. J. Lipps, *Nat. Struct. Mol. Biol.*, 2008, **15**, 598–604.
86 A. L. Moye, K. C. Porter, S. B. Cohen, T. Phan, K. G. Zyner, N. Sasaki, G. O. Lovrecz, J. L. Beck and T. M. Bryan, *Nat. Commun.*, 2015, **6**, 7643.
87 J. S. Smith, Q. Chen, L. A. Yatsunyk, J. M. Nicoludis, M. S. Garcia, R. Kranaster, S. Balasubramanian, D. Monchaud, M. P. Teulade-Fichou, L. Abramowitz, D. C. Schultz and F. B. Johnson, *Nat. Struct. Mol. Biol.*, 2011, **18**, 478–486.
88 S. Neidle, *FEBS J.*, 2010, **277**, 1118–1125.
89 C. B. Harley, A. B. Futcher and C. W. Greider, *Nature*, 1990, **345**, 458–460.
90 M. Z. Levy, R. C. Allsopp, A. B. Futcher, C. W. Greider and C. B. Harley, *J. Mol. Biol.*, 1992, **225**, 951–960.
91 F. Sampedro Camarena, G. Cano Serral and F. Sampedro Santaló, *Clin. Transl. Oncol.*, 2007, **9**, 145–154.
92 J. W. Shay, *Curr. Opin. Cell Biol.*, 2018, **52**, 1–7.
93 J. D. Henson, A. A. Neumann, T. R. Yeager and R. R. Reddel, *Oncogene*, 2002, **21**, 598–610.
94 S. E. Artandi and R. A. DePinho, *Carcinogenesis*, 2009, **31**, 9–18.
95 A. J. Cesare and R. R. Reddel, *Nat. Rev. Genet.*, 2010, **11**, 319–330.
96 S. Neidle, *Curr. Opin. Struct. Biol.*, 2009, **19**, 239–250.
97 S. Neidle, *Nat. Rev. Chem.*, 2017, **1**, 0041.
98 P. J. Campbell, *Cell*, 2012, **148**, 633–635.
99 Y. Xu, *Chem. Soc. Rev.*, 2011, **40**, 2719–2740.
100 W. Chen, Y. Zhang, H.-B. Yi, F. Wang, X. Chu and J.-H. Jiang, *Angew. Chem., Int. Ed.*, 2023, **62**, e202300162.
101 J. Weynand, A. Diman, M. Abraham, L. Marcélis, H. Jamet, A. Decottignies, J. Dejeu, E. Defrancq and B. Elias, *Chem. – Eur. J.*, 2018, **24**, 19216–19227.
102 K. Kawauchi, R. Urano, N. Kinoshita, S. Kuwamoto, T. Torii, Y. Hashimoto, S. Taniguchi, M. Tsuruta and D. Miyoshi, *Genes*, 2020, **11**, 1340.
103 E. Cadoni, L. De Paepe, G. Colpaert, R. Tack, D. Waegeman, A. Manicardi and A. Madder, *Nucleic Acids Res.*, 2023, **51**, 4112–4125.
104 S. N. Georgiades, N. H. Abd Karim, K. Suntharalingam and R. Vilar, *Angew. Chem., Int. Ed.*, 2010, **49**, 4020–4034.
105 M. R. Gill, J. Garcia-Lara, S. J. Foster, C. Smythe, G. Battaglia and J. A. Thomas, *Nat. Chem.*, 2009, **1**, 662–667.
106 T. Wilson, P. J. Costa, V. V. Félix, M. P. Williamson and J. A. Thomas, *J. Med. Chem.*, 2013, **56**, 8674–8683.
107 L. Holden, K. S. Gkika, C. S. Burke, C. Long and T. E. Keyes, *Inorg. Chem.*, 2022, **62**, 2213–2227.
108 A. De Cian, E. DeLemos, J. L. Mergny, M. P. Teulade-Fichou and D. Monchaud, *J. Am. Chem. Soc.*, 2007, **129**, 1856–1857.
109 W. J. Chung, B. Heddi, F. Hamon, M. P. Teulade-Fichou and A. T. Phan, *Angew. Chem., Int. Ed.*, 2014, **53**, 999–1002.
110 M. Vorlíčková, I. Kejnovská, K. Bednářová, D. Renčiuk and J. Kypr, *Chirality*, 2012, **24**, 691–698.
111 D. A. Case, H. M. Aktugla, K. Belfon, I. Y. Ben-Shalom, J. T. Berryman, S. R. Brozell, D. S. Cerutti, T. E. Cheatham III,

G. A. Cisneros, V. W. D. Cruzeiro, T. A. Darden, N. Forouzesh, G. Giambaşu, T. Giese, M. K. Gilson, H. Gohlke, A. W. Goetz, J. Harris, S. Izadi, S. A. Izmailov, K. Kasavajhala, M. C. Kaymak, E. King, A. Kovalenko, T. Kurtzman, T. S. Lee, P. Li, C. Lin, J. Liu, T. Luchko, R. Luo, M. Machado, V. Man, M. Manathunga, K. M. Merz, Y. Miao, O. Mikhailovskii, G. Monard, H. Nguyen, K. A. O'Hearn, A. Onufriev, F. Pan, S. Pantano, R. Qi, A. Rahnamoun, D. R. Roe, A. Roitberg, C. Sagui, S. Schott-Verdugo, A. Shajan, J. Shen, C. L. Simmerling, N. R. Skrynnikov, J. Smith, J. Swails, R. C. Walker, J. Wang, J. Wang, H. Wei, X. Wu, Y. Wu, Y. Xiong, Y. Xue, D. M. York, S. Zhao, Q. Zhu and P. A. Kollman, *Amber22 and AmberTools22*, University of California, San Francisco, 2022..

112 Y. Wang and D. J. Patel, *Structure*, 1993, **1**, 263–282.

113 J. P. Hall, K. O'Sullivan, A. Naseer, J. A. Smith, J. M. Kelly and C. J. Cardin, *Proc. Natl. Acad. Sci. U. S. A.*, 2011, **108**, 17610–17614.

114 H. Niyazi, J. P. Hall, K. O'Sullivan, G. Winter, T. Sorensen, J. M. Kelly and C. J. Cardin, *Nat. Chem.*, 2012, **4**, 621–628.

115 J. P. Hall, P. M. Keane, H. Beer, K. Buchner, G. Winter, T. L. Sorensen, D. J. Cardin, J. A. Brazier and C. J. Cardin, *Nucleic Acids Res.*, 2016, **44**, 9472–9482.

116 J. Weiser, P. S. Shenkin and W. C. Still, *J. Comput. Chem.*, 1999, **20**, 217–230.

117 M. G. Walker, P. J. Jarman, M. R. Gill, X. Tian, H. Ahmad, P. A. N. Reddy, L. McKenzie, J. A. Weinstein, A. J. H. M. Meijer, G. Battaglia, C. G. W. Smythe and J. A. Thomas, *Chem. – Eur. J.*, 2016, **22**, 5996–6000.

118 Z. Zhou, J. Liu, T. W. Rees, H. Wang, X. Li, H. Chao and P. J. Stang, *Proc. Natl. Acad. Sci. U. S. A.*, 2018, **115**, 5664–5669.